MODELING THE CHEMICAL AND PHOTOPHYSICAL PROPERTIES OF GOLD COMPLEXES

Khaldoon A. Barakat, B.S.

Thesis Prepared for the Degree of

MASTER OF SCIENCE

UNIVERSITY OF NORTH TEXAS

August 2004

APPROVED:

Thomas R. Cundari, Major Professor
Mohammad A. Omary, Committee Member
Ruthanne D. Thomas, Chair of the Department of Chemistry
Sandra L. Terrell, Dean of the Robert B. Toulouse School of Graduate Studies

Barakat, Khaldoon A., Modeling the chemical and photophysical properties of gold complexes. Master of Science (Inorganic Chemistry), August 2004, 31 pp., 3 tables, 11 illustrations, references, 34 titles.

Various gold complexes were computationally investigated, to probe their photophysical, geometric, and bonding properties. The geometry of Au^{I} complexes (ground state singlet) is very sensitive to the electronic nature of the ligands: σ-donors gave a two-coordinate, linear shape; however, π-acceptors yielded a three-coordinate, trigonal planar geometry. Doublet $Au^{II}L_3$ complexes distort to T-shape, and are thus ground state models of the corresponding triplet $Au^{I}L_3$. The disproportionation of $Au^{II}L_3$ to $Au^{I}L_3$ and $Au^{III}L_3$ is endothermic for all ligands investigated, however, σ-donors are better experimental targets for Au^{II} complexes. For dimeric Au^{I} complexes, only one gold center in the optimized triplet exciton displays a Jahn-Teller distortion, and the Au---Au distance is reduced versus the ground state distance (*i.e.*, two reasons for large Stokes' shifts).

ACKNOWLEDGEMENTS

The author wishes to acknowledge the generous donation of the MOE program by the Chemical Computing Group, Inc., Montreal, Canada. The National Science Foundation is acknowledged for partial support of this research.

TABLE OF CONTENTS

LIST OF TABLES

LIST OF ILLUSTRATIONS

CHAPTER 1

INTRODUCTION

Heavy metal complexes play a very important role in relativistic quantum chemistry, both as targets for the development and testing of novel methods and as textbook model representations. In fact, heavy metals like gold and mercury exhibit some of the largest relativistic effects,[1,2] owing in part to the presence of spin-orbit coupling, which is largely due to their high atomic mass. Pyykkö have stated that relativity is one of the basic theories of modern physics, in addition to being very essential for producing highly accurate results in quantum chemistry.[1] Relativistic effects in chemistry arise from the high speeds of electrons moving near a heavy nucleus, and increase roughly as Z^2, (Z = nuclear charge).[1,2] Gold has Z = 79, being a third row transition metal in the periodic table of the elements, and hence relativistic effects in gold chemistry are very prominent, yielding the so-called "gold maximum".[1] Some of the best illustrations of the relativistic consequences in gold chemistry can be seen in the phosphorescence and geometric properties of gold complexes, and indeed even the characteristic yellow color of elemental gold.[1]

Photoluminescence refers to fluorescence or phosphorescence emissions, and is due to a photophysical process. Fluorescence results from a radiative transition between two states of same spin multiplicity, which is different from phosphorescence where the radiative transition is between two states of different spin multiplicity. For a photophysical transition to occur, a discrete quantum of light (photon), of the appropriate wavelength and energy should be absorbed, thus causing the molecule to gain a surplus of energy, and resulting in the formation of an energetically unstable state (electronically excited state or exciton) relative to the ground state

of the molecule. The exciton may subsequently undergo chemical reaction, or just dispel its energy by a photophysical progression of deactivation (non-radiative or radiative processes).

The radiative transitions that result are allowed, or forbidden, depending on whether they obey certain factors known as the selection rules. These selection rules can be violated in the presence of significant spin-orbit coupling as is observed for heavy elements like gold. One of the examples of violating the selection rules is in phosphorescence. To illustrate, a spin-forbidden triplet to singlet transition may occur in the phosphorescence of some gold compounds, however, this transition is 'weakly allowed'. This weakly allowed transition is relatively slow and thus may persist for several seconds subsequent to the cessation of irradiation. This process is termed phosphorescence.

Gold complexes, especially the +1 formal oxidation state (Au^I), have attracted the attention of many scientists to this field of chemistry. Luminescent Au^I compounds are of interest in terms of application as light emitting devices or diodes (LEDs). Balch *et al.* have demonstrated that compounds such as the gold(I) trimer (gold,tris[μ-[methoxy(methylimino)methyl]]) $[Au_3(MeN{=}COMe)_3]$, display solvo-luminescence;[3] after irradiation with near-UV light, the trimer exhibits detectable photoluminescence for several seconds after termination of irradiation, and then subsequently upon contact with solvent.[3] Au(I) complexes most commonly exist as Au^IL_2 (L = ligand) species, however Au^IL_3 and Au^IL_4 species are also known.[4] For their part, Gimeno and Laguna in 1997, published a chemical review on the study of three- and four-coordinate gold(I) complexes, where the tendency of Au^I to form two-coordinate complexes versus its isoelectronic centers like Ag and Hg was emphasized, although other coordination numbers such as trigonal planar and T-shaped may exist.[4] The photoluminescence properties of these species differ from one coordination mode to

another, for example, $Au^{I}L_2$ complexes display luminescence only in the presence of Au···Au (aurophilic) interactions, while $Au^{I}L_3$ complexes exhibit luminescence with and without Au···Au interactions.[5,6,7]

Gray and McCleskey studied the emission spectroscopic properties of 1,2-bis(dicyclohexylphosphino)ethane complexes of Gold(I) in 1992, and proposed that the depopulation of the highest occupied molecular orbital (HOMO), and the population of the lowest unoccupied molecular orbital (LUMO), causes the bond between the gold and the ligand (Au-L) in the complex to become shorter and stronger.[5] Another of the many experimental studies of the photoluminescence of Au^{I} in solution was the work of Fackler and coworkers, where the photoluminescence of gold(I) phosphine complexes in aqueous solution was carried out in 1995.[6] Fackler *et al.* proposed that for trivalent gold phosphine complexes, the geometry around the gold center in solution is trigonal planar, and that the emissive state is a triplet excited state.[6] In 1976, Hoffman *et al.* performed theoretical and experimental investigations of trialkyl Au^{I} species, in particular the three coordinate trimethylgold complex, and concluded that trigonal geometry distortion to T-shaped is feasible.[8]

The chemistry of gold is dominated by the +1 and +3 formal oxidation states, while the +2 formal oxidation state is rare. Despite this, the number of experimentally characterized complexes of Au^{II} has increased noticeably during the past decade.[9] The scarce presence of Au^{II} compounds in the experimental literature, especially for monometallic species, makes theoretical investigations of Au^{II} very attractive. Au^{II} has 9 electrons in the valence 5d subshell, thus the presence of an odd electron has been identified by Laguna as one of the causes for the poor stability of its compounds.[9] In general, both Au^{I} and Au^{III} complexes are closed-shell, diamagnetic species, while Au^{II} complexes are paramagnetic. However, according to results

obtained by investigating the first and second ionization energies of gold, silver, copper, and mercury, Au^{II} complexes should be easier to stabilize than those of Ag^{II}, where the latter can be prepared but are very potent oxidizing agents.[1,10] Stace *et al.* have reported the successful formation of stable Au^{II} complexes in the gas-phase with ligands that are good σ donor-π acceptor molecules, such as pyridine (C_5H_5N), acetonitrile (CH_3CN), and acetone (C_3H_6O).[10] However, σ-only donor ligands like water (H_2O) and ammonia (NH_3) did not form stable Au^{II} compounds. Only a limited number of monometallic Au^{II} complexes have been structurally characterized, for example, the mononuclear $[Au^{II}([9]aneS_3)_2](BF_4)_2$ that was obtained by reduction of $HAu^{III}Cl_4{\cdot}3H_2O$ with two equivalents of $[9]aneS_3$ in refluxing HBF_4/MeOH.[11] Calculations on Au^{II} complexes are likewise rare. Previously, Barakat *et al.* conducted calculations on the $[Au(PH_3)_3]^{+2}$ model and suggested that this monomer exhibited the same distortion to T-shape (*i.e.*, P-Au-P ~ 90° and 180°) as the triplet excited state of $[Au(PH_3)_3]^{+}$.[12]

Many Au^{I} dimers have been characterized by crystallography and found to have short Au···Au interactions.[9] Au^{I} dimers have been found to exhibit attractive (aurophilic) interactions between the closed-shell d^{10} cations. Pyykkö and Mendizabal have studied the d^{10}-d^{10} closed-shell attraction computationally, and reported that the presence of a bridging ligand in the case of intramolecular interactions, aids this type of interactions.[13] Yam *et al*. concluded that the interesting photoluminescence properties of Au^{I} dimers,[14] as well as medical uses,[4] such as antitumor drugs and photodynamic therapeutic agents, have spurred a rapid increase in research on gold chemistry.[4,13,14,15]

In order to develop gold-based materials with superior photochemical efficiencies, it is paramount to understand the fundamental nature of the luminescent excited state in gold complexes, and to unravel factors that influence the geometry and bonding properties of gold

compounds. In this computational research, a study of the bonding, structure, energetics, and spectroscopy of different ground and excited states of gold compounds was carried out. Also, the effect of σ donor, or π donor/acceptor ligands on the coordination chemistry of Au^{I}, Au^{II}, Au^{III} and Au^{I}-dimers, was inspected, in addition to examining whether different ligands affect the coordination geometry of the gold centers involved.

CHAPTER 2

COMPUTATIONAL METHODS

2.1 Quantum Mechanical (QM) Calculations

Monomer models studied were $[Au^{Z}L_3]$ (Z = I, II, III; L = PH_3, H_3C-C≡N (acetonitrile), H_3C-N≡C (methylisonitrile), H-C≡N, CO, pyridine, and terpyridine (terpy). The dimer models, $[Au^{I}_2(PH_2(CH_2)_xPH_2)_3]^{+2}$ (x = 1, 2), studied were of two isomers: closed and open (see Figure. 1).

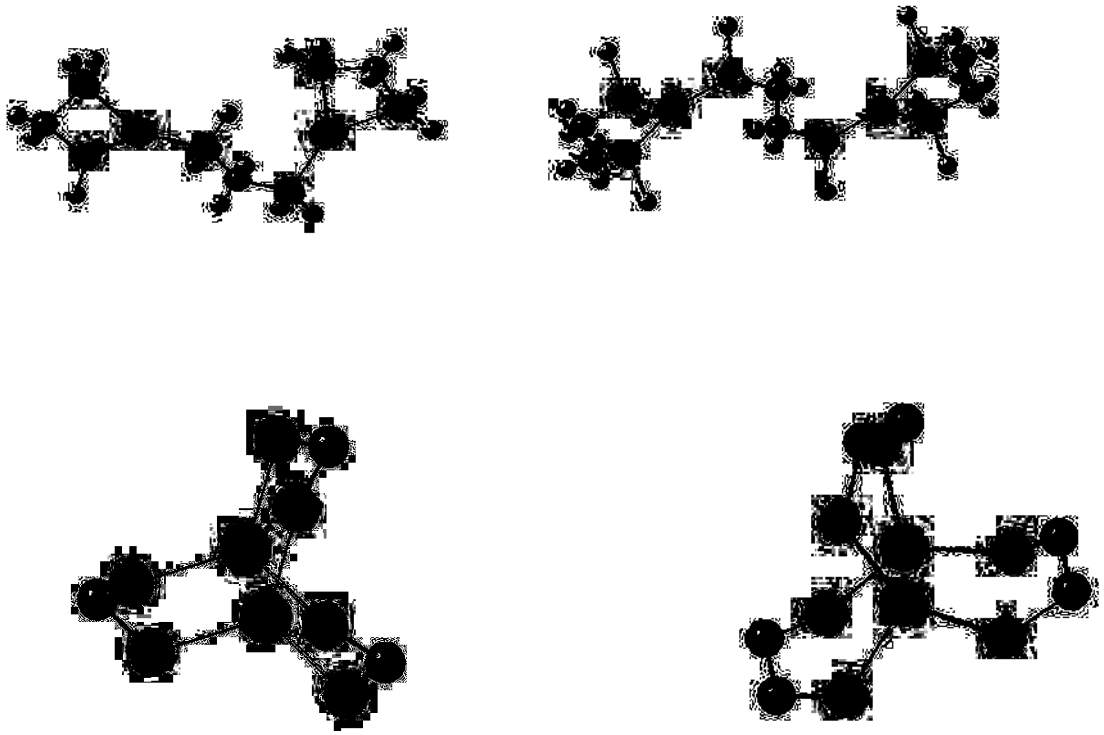

Figure 1. Au^{I}-dimer models, open (top) and closed (bottom) isomers; hydrogen atoms omitted from closed isomer for clarity.

2.1.1 Methods

Calculations were performed using density functional theory (DFT),[16] specifically the B3PW91 hybrid functional.[17] The method was selected based on a series of test calculations on the ground state singlet and excited state triplet of $[Au(PH_3)_3]^+$, using different methodologies with progressing basis sets, see Table 1.

2.1.2 Basis Sets

The LANL2DZ effective core potentials and valence basis set[18] were used in conjunction with Pyykkö and Mendizabal suggested two f-type polarization functions with the exponents 0.2 which is needed in describing the metallophilic attraction, and 1.19 that is needed in describing the covalent bonds,[13] and the Couty-Hall p-type functions[19] to describe the valence electrons of gold. Main group elements were described with the LANL2DZ basis set augmented with a d polarization function. This level of theory was used in a previous study of Au^I photochemistry where the phosphorescent excited state of three-coordinate Au^I phosphine complexes was investigated.[12]

Geometries were optimized for the singlet ground state of Au^I complexes, doublet ground state of Au^{II} complexes, singlet ground state of Au^{III} complexes, and the singlet ground and triplet excited states of Au^I-dimer complexes. Full geometry optimizations without any metric or symmetry restrictions were employed to obtain the minima in this research. All of the resultant stationary points were characterized as true minima (*i.e.*, no imaginary frequencies) by calculation of the energy Hessian. Closed- and open-shell species were described with the restricted and unrestricted Kohn-Sham formalisms, respectively, with no evidence of spin contamination for the latter.

2.2 Hybrid Quantum Mechanical/Molecular Mechanical (QM/MM) Calculations

The Au^{II} complexes $[Au^{II}L_3]^{+2}$ (L = PMe_3, PPh_3, $PPhCy_2$, and $(TPA)_3$, TPA = tris(1,3,5-triaza-7-phosphaadamantane), as shown in (figure. 2),

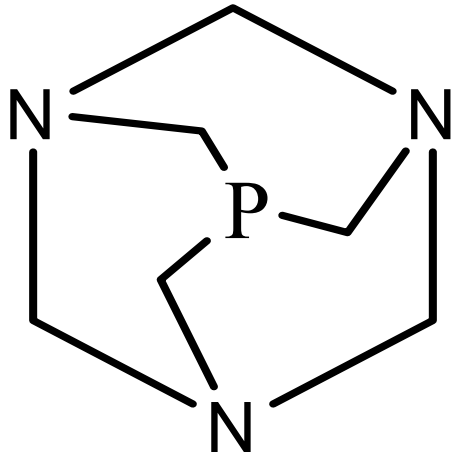

Figure 2. TPA = tris(1,3,5-triaza-7-phosphaadamantane).

were studied with hybrid QM/MM techniques employing the ONIOM methodology.[20] In QM/MM calculations, QM and MM are combined into one calculation where one region of the molecule is modeled using QM, this is especially useful for very large compounds. The QM region in this research contained Au and the three phosphorus atoms; DFT using the B3PW91 hybrid functional and the same augmented LANL2DZ basis set as described above in section 2.1.2 was employed for the QM core. The MM region included the rest of the molecule, *i.e.*, bulky hydrocarbyl (R) groups on the phosphorus atoms, which were modeled with the Universal Force Field (UFF).[21] All $[Au^{II}L_3]^{+2}$ geometries were fully optimized, without any symmetry constraints. The Opt=NoMicro option was used to prevent microiterations during the optimization steps.

All QM and QM/MM calculations were performed using the Gaussian 98 suite of programs.[22] The models for L = PMe_3, PPh_3, and TPA were built from scratch using the *GaussView* program.[23] For $[Au(PPhCy_2)_3]^{+2}$, the initial guess structure was built using the Spartan program,[24] then a conformational search was conducted (keeping the AuP_3 core fixed) using the Hybrid Monte Carlo conformational search algorithm in the MOE program.[25] The conformational search was run for 1 ps at 300 K with a time step of 5 fs. Two thousand snapshots were collected, and then the lowest steric energy conformer was extracted and used for subsequent QM/MM calculations with Gaussian98.

2.3 Geometry Scan Calculations

In addition to full geometry optimizations, a scan calculation of the angle Φ (see Figure. 3) was done using the model $[Au(PH_3)_3]^+$ to inspect the out-of-plane bending of the AuP_3 unit that occurred in some of the Au^I complexes studied.

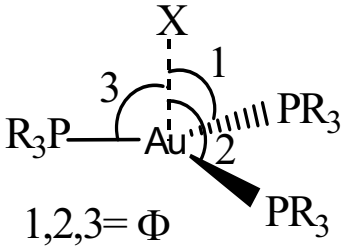

Figure 3. Definition of the Φ (out-of-plane bending) angle for three-coordinate gold complexes.

Starting with the fully optimized singlet global minimum of $[Au(PH_3)_3]^+$ the bond angle P-Au-X, where X is a ghost atom on the three-fold symmetry axis, was varied in 4° increments from 90° to 110°. The time-dependent DFT method[26] was used to calculate the singlet-triplet transition in this scan calculation. Previous scan calculations investigated the response of the singlet-triplet energy gap to varying the Au-P bond lengths and the P-Au-P bond angles.[12]

CHAPTER 3

RESULTS AND DISCUSSION

3.1 $Au^{I}L_3$ Complexes

3.1.1 Effect of Out-of-Plane Distortion on Stokes' Shift

Barakat *et al.* have reported that to obtain accurate photochemical results, the triplet excited state of $[Au(PR_3)_3]^+$ must be dealt with as a different entity that is geometrically distinct from the ground state.[12] The B3PW91 functional was used in conjunction with the Los Alamos relativistic pseudopotentials[18] to study the ground state singlet and lowest energy triplet states of $[Au(PR_3)_3]^+$ models with different R groups (R_3 = $(H)_3$, $(CH_3)_3$, $(Ph)_3$, $(Ph)(Cy)_2$, and TPA). The results indicated that the triplet exciton exhibits a Jahn-Teller distortion from trigonal planar (P-Au-P ~ 120º) towards T-shaped (P-Au-P ~ 90º and 180º), as opposed to the bond distance (Au-P) change previously proposed in the experimental literature.[5,6] Calculations provided an explanation for the large experimental Stokes' shifts.[5,6] When larger, more sterically hindered R groups were used, the distortion from trigonal planar towards the T-shape geometry was lessened in response to R···R steric repulsion among the approximately *cis* phosphines of the T-shaped geometry of triplet $[Au(PR_3)_3]^+$.

There was also a noticeable out-of-plane bending in the triplet exciton of $[Au(PR_3)_3]^+$ as the R group got larger (see Figure. 4).[12] Barakat *et al.* reported that the major excited state distortion mode responsible for the Stokes' shift is a P-Au-P angular change, not an Au-P bond distance change (see Figure. 5 and 6).[12] The scan of Φ done in the present research reinforced the previous results, because as the three Φ angles (see Fig. 3) were varied from 90˚ (trigonal planar geometry) to 110˚ (*ca.* tetrahedral geometry), the emission wavelength varied from (269 nm) to (351 nm), respectively, which was still not in the visible region even for a full tetrahedral

distortion. Moreover, the actual out-of-plane bending observed in the calculated $[Au(PR_3)_3]^+$ models did not distort all the way to a tetrahedral geometry (see Figure. 7). A similar trend was seen previously for the Au-P bond length scan. As the Au-P bond was scanned between 2.50 Å and 2.70 Å for the triplet $[Au(PR_3)_3]^+$ while holding the model at the trigonal planar geometry, the wavelength varied from (262 nm) to (310 nm), respectively. However, the change of the angle Θ (P-Au-P angles) from the trigonal planar geometry to the T-shape results in an emission wavelength shift into the visible region (~ 416 nm), which is comparable to experimental measurements.[5,6] Thus, it is concluded on the basis of the present calculations that the Stokes' shift is primarily due to P-Au-P angular distortion as opposed to Au-P bond length changes or out-of-plane bending of the gold coordination environment.

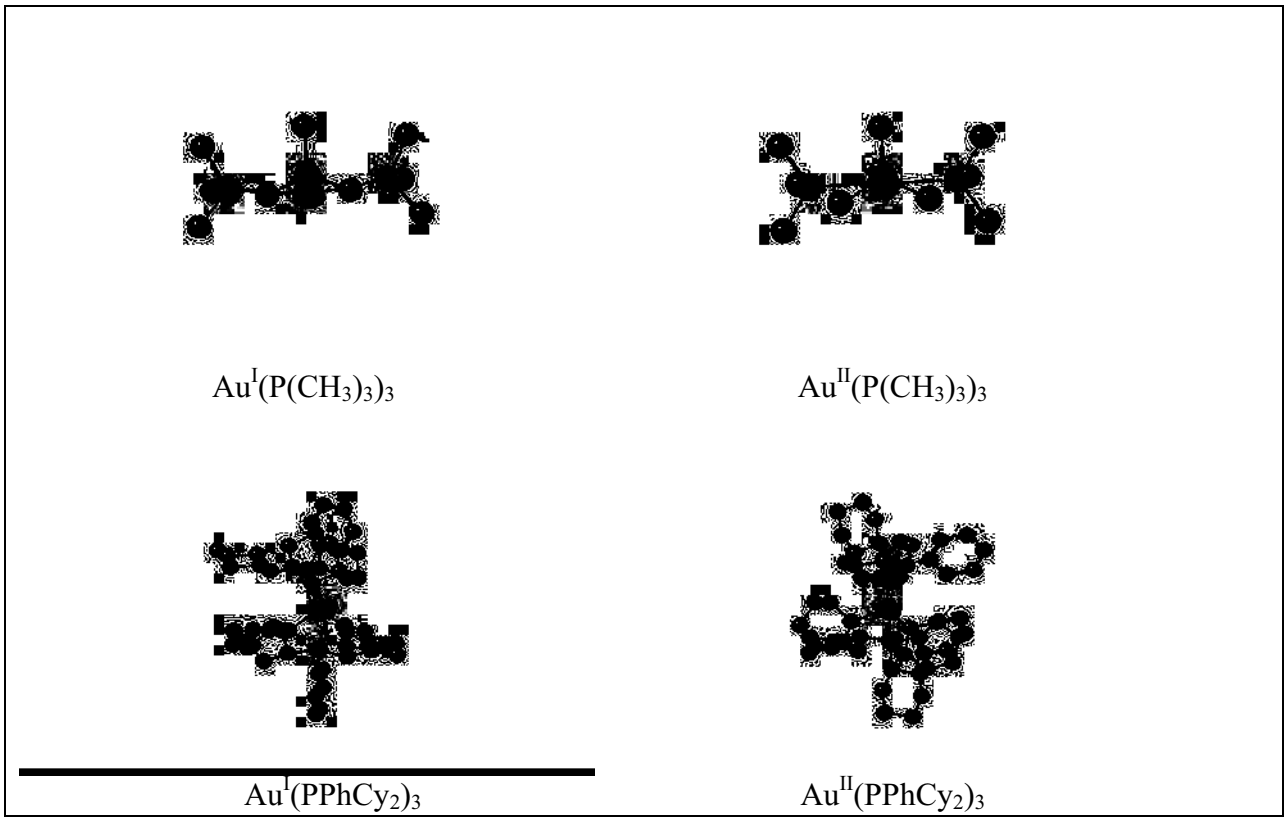

Figure 4. Au^{I} and Au^{II} models showing out-of-plane bending, (left) for Au^{I}, and (right) for Au^{II}. ($PhCy_2$ = phenyldicyclohexyl).

3.1.2 Non-Phosphine $Au^{I}L_3$ Complexes

Previous work focused on phosphine complexes, for their prospective applications for a variety of techniques.[4,12,14] However, there is considerable experimental research on the photophysical properties of Au^{I} with other ligands.[3,9] In this project, $[Au^{I}L_3]^+$ was modeled with L = H-C≡N, H_3C-C≡N (acetonitrile), H_3C-N≡C (methylisonitrile), CO, pyridine, and terpyridine (terpy), most of which $Au^{I}L_3$ complexes are not known (*i.e.*, methylisonitrile). From the results in Table 2 for singlet $[Au^{I}L_3]^+$ it is found that the ligands split into two groups - σ-donor ligands (H-C≡N, H_3C-C≡N, and pyridine), and π-acceptor ligands (H_3C-N≡C and CO).

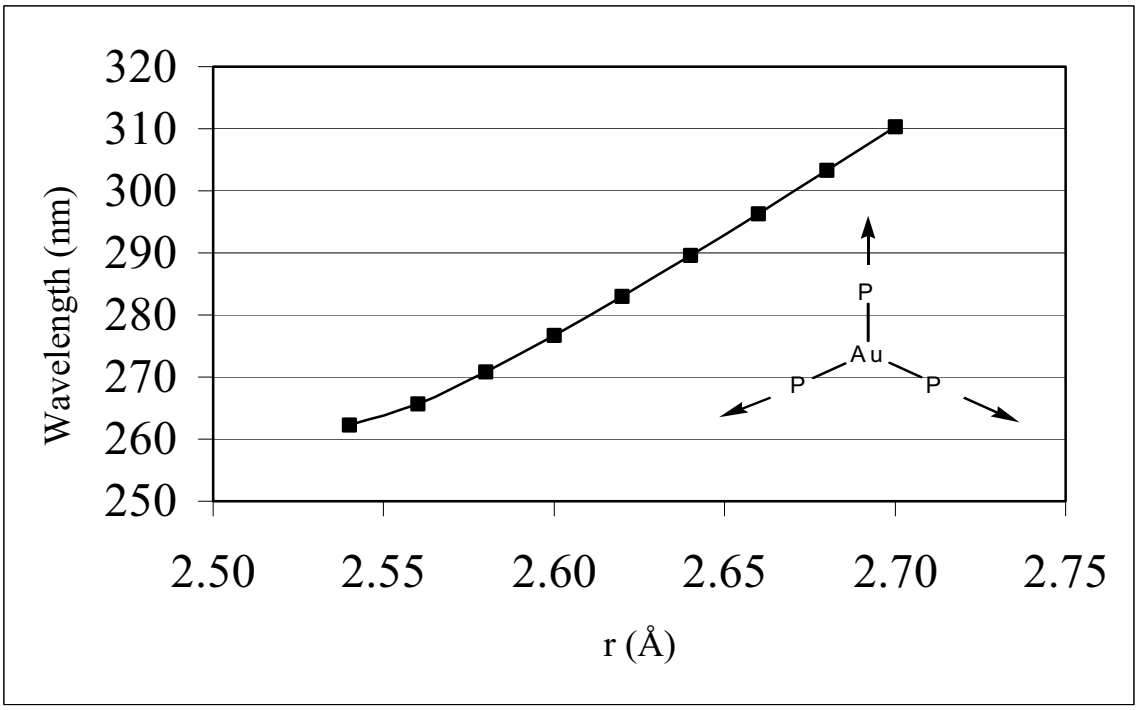

Figure 5. Scan calculation showing effect of changing Au-P bond length on singlet-triplet transition wavelength of $[Au(PH_3)_3]^+$.

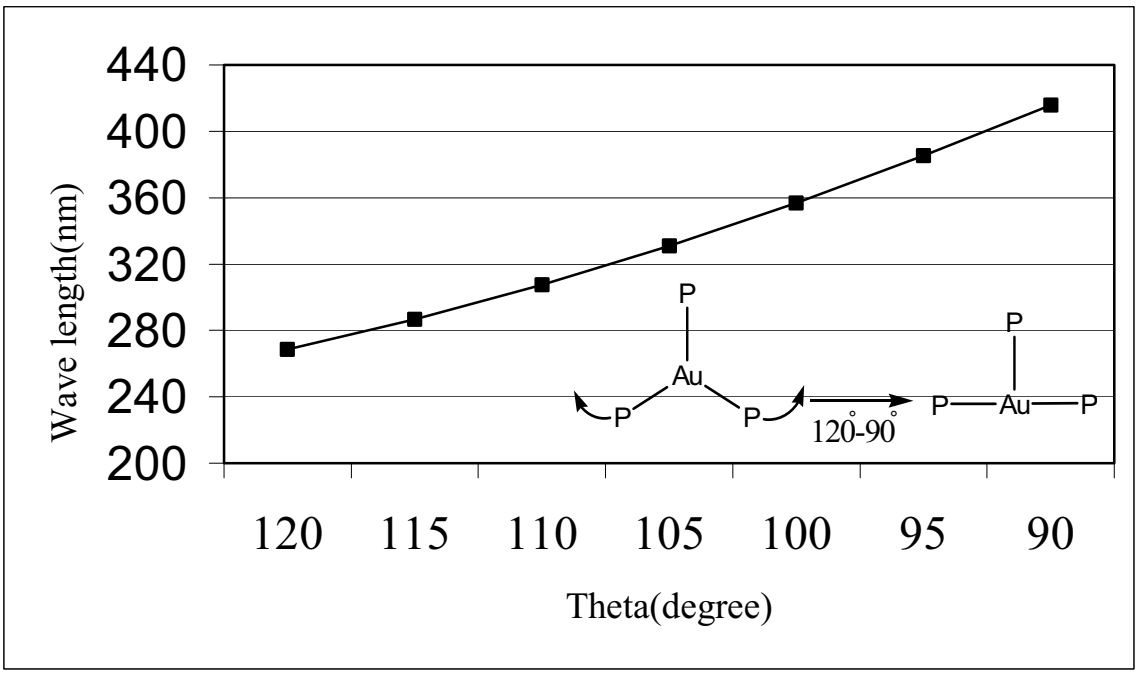

Figure 6. Scan calculation showing effect of changing P-Au-P bond angle (θ) on singlet – triplet transition wavelength of $[Au(PH_3)_3]^+$.

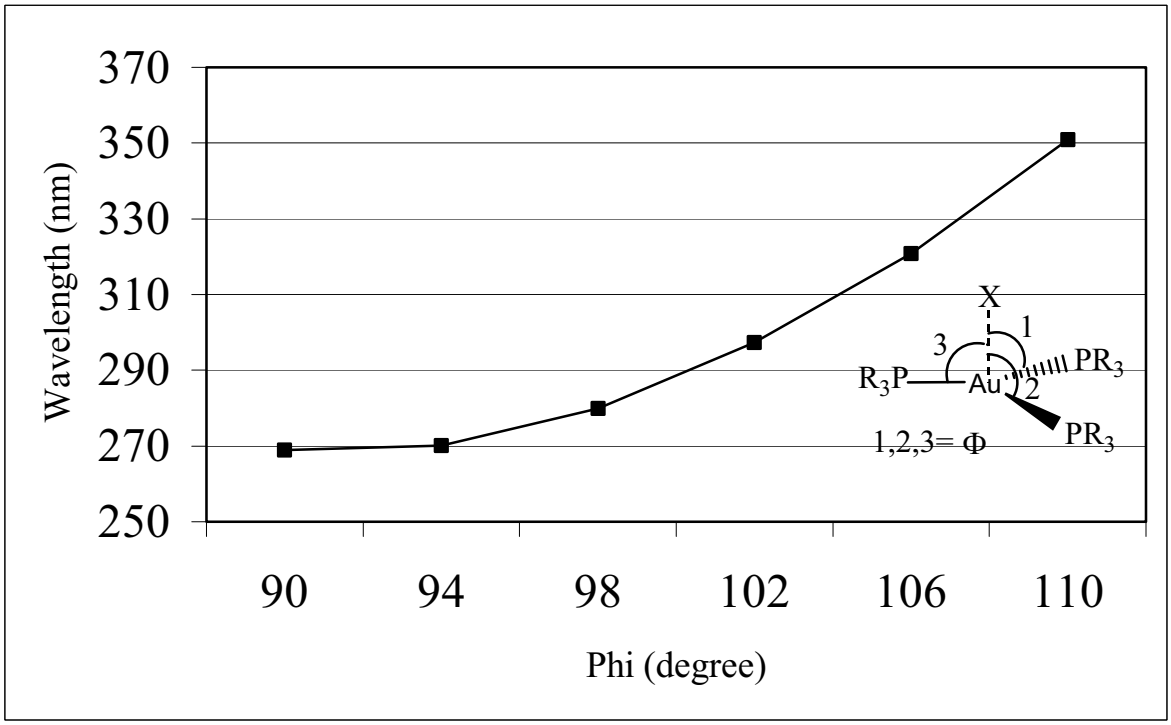

Figure 7. Scan calculation showing effect of changing Φ angle on singlet – triplet transition wavelength of $[Au(PH_3)_3]^+$.

The σ-donor ligands group has "T-shape" geometry, or more accurately they correspond to linear, two-coordinate Au^I complexes with the third ligand (orthogonal to the other two ligands) being only very weakly ligated. The $[Au^IL_3]^+$ complexes with π-acceptor ligands, phosphines included, on the other hand are trigonal planar. The origin of this geometric difference is electronic rather than steric, which can be seen when the ground state geometries are compared for the isosteric acetonitrile (σ-donor) and methylisonitrile (π-acceptor) ligands, Table 2.

Recall that Au^IL_2 complexes are nonluminescent in the absence of aurophilic interactions, while Au^IL_3 complexes are luminescent.[5,6,7] Hence, the existence of a geometric continuum from linear two-coordinate to trigonal planar three-coordinate could have important ramifications for luminescent Au^I materials with large (and easily tunable) Stokes' shifts, for which a T-shaped geometry can be thought of as a point along this hypothetical reaction coordinate. The possibility of geometries intermediate between two and three coordination was investigated by analyzing the series of complexes, $[Au(N{\equiv}C\text{-}Me)_x(C{\equiv}N\text{-}Me)_{3-x})]^+$ for x = 0, 1, 2, 3. It was found that an σ-donor acetonitrile ligand (if present) was dissociated from the complex leading to the formation of a linear, two-coordinate Au^I complex, while the π-acceptor isonitrile ligands always remain bonded to the Au atom, see Table 2. Furthermore, the geometries of the complexes that contained the σ-donor acetonitrile ligands resulted in formation of two coordinate Au^I complexes. Hence, no geometries intermediate of either the trigonal planar and/or T-shaped were found through this computational exercise.

3.2 Au^{II} Complexes

Mononuclear Au^{II} complexes are rare in comparison to Au^I and Au^{III} complexes.[10] Most examples that are known are binuclear complexes for which the presence of two transition metals

can make the assignment of a formal oxidation state ambiguous. However, Stace *et al.* suggested that the Au^{II} oxidation state may exist as: (a) a transient intermediate in the redox reaction between Au^{I} and Au^{III}; (b) in mononuclear complexes where a good σ donor- π acceptor ligand can stabilize the metal.[10] Laguna *et al.* have reported that there is a strong tendency for disproportionation from Au^{II} to give Au^{I} and Au^{III}.[9]

Previous reports of calculations suggested that a ground-state d^9-$[Au^{II}(PH_3)_3]^{+2}$ species should also exhibit a similar Jahn-Teller distorted T-shaped geometry as the triplet excited state of the Au^{I} congener.[12] Hence, Au^{II} complexes represent interesting targets in the study of luminescent materials as ground state models of the triplet exciton of Au^{I} complexes. As experimental studies of mono-metallic Au^{II} complexes are rare, computational studies were undertaken to investigate their coordination chemistry, in particular phosphine complexes of Au^{II}.

QM/MM calculations on the doublet $[Au(PR_3)_3]^{+2}$ model showed that it distorted to a T-shape geometry. However, the out-of-plane bending that was obvious with the largest R groups for triplet $[Au(PR_3)_3]^{+}$ was reduced in analogous Au^{II} complexes with the same R groups (see Figure. 4). Also, the distortion towards the T-shape for Au^{II} was less than that previously found[12] for triplet Au^{I} as shown in (Figure. 8). For example, the P-Au-P angles varied from P-Au-P = 95˚, 174˚, 88˚ (P-Au-P angle sum = 357˚) for the triplet $[Au(TPA)_3]^{+}$ to P-Au-P = 103˚, 162˚, 95˚ (sum = 360˚) for doublet $[Au(TPA)_3]^{+2}$. Note that for a perfectly planar arrangement of ligating atoms the sum of the angles about the central gold atom will be 360°. For the other doublet $[Au(PR_3)_3]^{+2}$ complexes the P-Au-P angle sums for the ligands R_3 = $(CH_3)_3$, $(Ph)_3$, and $(Ph)(Cy)_2$, were 343˚, 341˚ and 352˚, respectively,[12] for triplet exciton of the Au^{I} complexes; for

the doublet Au^{II} tris-phosphine complexes, the P-Au-P angle sum is 360˚ (planar) for all three phosphines.

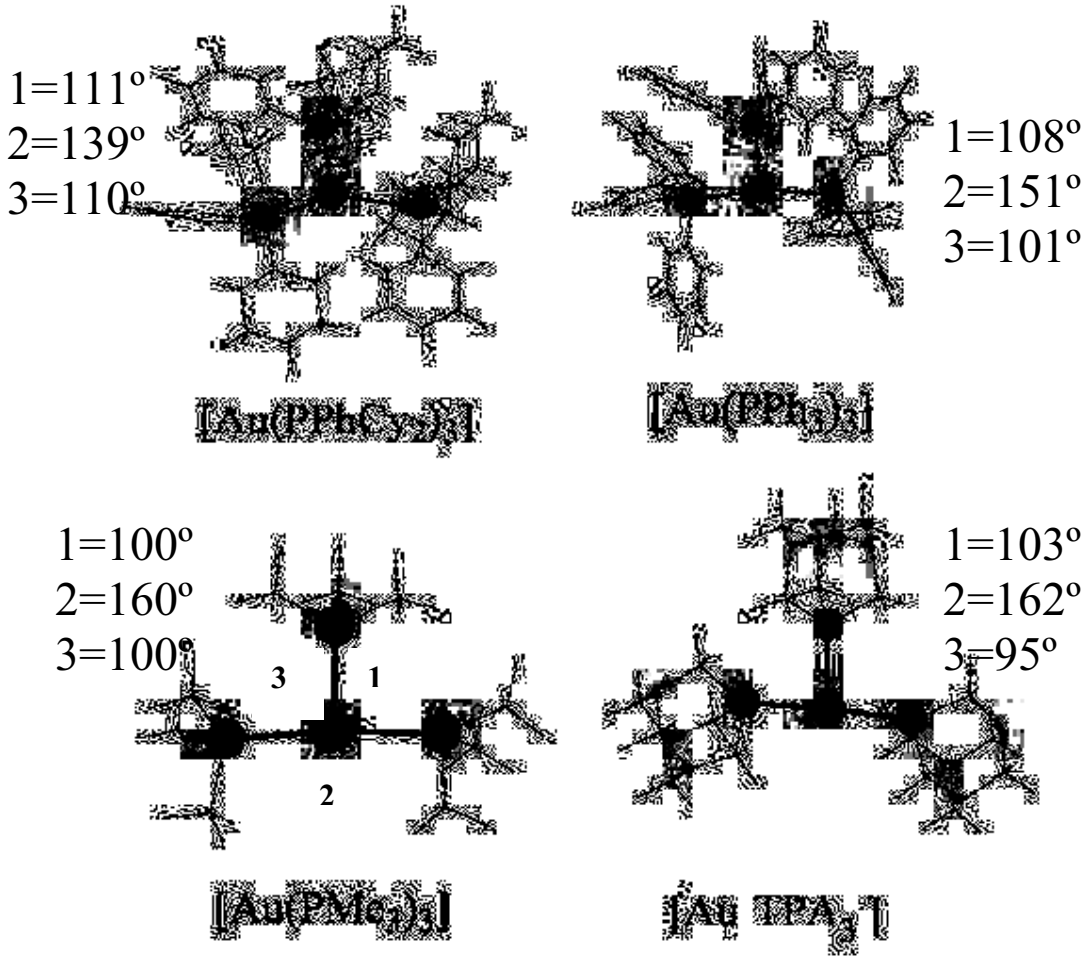

Figure 8. QM/MM optimized structures of doublet $[Au(PR_3)_3]^{+2}$ models.

Quantum mechanical calculations for complexes with non-phosphine ligands for $[Au^{II}L_3]^{+2}$ (L = H-C≡N, H_3C-N≡C, CO, and terpy) showed that the Au^{II} complex will distort towards a T-shape with Au-L bond lengths and L-Au-L bond angles as given in Table 2. The bond angles vary from (80°, 160°, 80°) for L = terpy, to (95°, 170°, 95°) for L = H-C≡N. Note

that unlike the singlet $Au^{I}L_3$ complexes, the T-shape is obtained for the corresponding Au^{II} complexes regardless of whether the ligands are σ-donors or π-acceptors. As disproportionation to Au^{I} and Au^{III} has been proposed as an important decomposition pathway for Au^{II} complexes,[9] a study of this reaction is of interest and was undertaken. Since the thermodynamic driving force for disproportionation (*i.e.*, 2 $Au^{II}L_3 \rightarrow Au^{I}L_3 + Au^{III}L_3$) becomes more endothermic/less exothermic one would expect that such ligands would be more viable candidates for the isolation of stable, monometallic Au^{II} complexes.

B3PW91/ (LANL2DZ, plus 2f-type[13] and p-type[19] functions on Au) calculations were carried out for $[AuL_3]^{+1,+2,+3}$ models for L = H-C≡N, H_3C-C≡N, H_3C-N≡C, CO, and terpy. The results in Table 2 show that the singlet Au^{III} complex angles were closer to a T-shape than for the doublet Au^{II}, especially for methylisonitrile and CO, where the angles when methylisonitrile was the ligand were (97°, 166°, 97°) for Au^{II}, (92°, 176°, 92°) for Au^{III}, and when CO was the ligand, the angles were (96°, 168°, 96°) for Au^{II}, (90°, 179°, 90°) for Au^{III}. The complexes of Au^{III} are very commonly found with a square planar coordination environment,[27] and hence these three-coordinate complexes can be thought of as square planar complexes with a vacant coordination site.

The ionization potential of atomic Au^{II} to Au^{III} has been measured in the gas-phase[28] as 34.0 eV. This experimental estimate is in good agreement with a calculated value of 33.1 eV found using the same basis sets and B3PW91 functional employed throughout this research for gold complexes. Indeed, this agreement is superior to that achieved using the same basis sets and performing the calculation at the more expensive coupled clusters level of theory, IP_3(CCSD(T)) = 32.9 eV. Using the experimental ionization potentials yields a gas-phase estimate of the

disproportionation reaction, equation 1, of 13.5 eV, compared to calculated estimates of 12.3 eV (B3PW91)

$$2\ Au^{II} \leftrightarrow\ Au^{I}\ +\ Au^{III} \qquad (1)$$

and 12.9 eV (CCSD(T)). Perhaps more interesting in the present context is the very large solvent effect on this reaction, which should more closely mimic a solution-phase redox process, ΔE_{disp} = 5.1 eV (B3PW91, PCM (PCM = polarizable continuum models),[29] solvent = water). The shift upon going from gas to solution phase is due to the very large stabilization of the Au^{III} atomic ion. Investigating the disproportionation reaction as a function of ligand, equation 2, indicates that the reaction is unfavorable for all ligands investigated, ΔE_{disp} (B3PW91, PCM, solvent = water, eV) = +2.5 (terpyridine), +2.0 (acetonitrile), +0.9 (PH_3), +1.7 (methylisonitrile), +1.4 (CO). The lack of experimental data makes the foregoing estimates of unknown accuracy, although the relative values are expected to be more reliable. However, the aforementioned relative values place the σ-donor ligands (*i.e.*, terpyridine) in the more (endothermic) reactions with the higher ΔE_{disp}, when compared to the π-acceptor ligands like PH_3, shifting the reaction in equation 2 to the left.

$$2\ Au(II)L_3 \leftrightarrow Au(I)L_3\ +\ Au(III)L_3 \qquad (2)$$

Thus, given the recent gas-phase experiments of Stace *et al.*,[10] plus the present calculations, Au^{II} complexes with σ-donor ligands especially terpyridine, would seem to be worthy targets for increased experimental study.

3.3 Au^I-Dimers

The Au^I dimer models $[Au_2(PH_2(CH_2)_{1,2}PH_2)_3]^{+2}$ exist in two isomeric forms - closed and open (see Figure. 1). A crystal structure was reported for $[Au_2(PR_2CH_2PR_2)_3]^{+2}$ where R= CH_3.[30] Geometry optimizations were done on the singlet ground state for both isomers, while the lowest energy triplet excited state was also geometry optimized for the closed isomer; the B3PW91 energies are reported in Table 3. For the two singlet ground states of closed $[Au_2(PH_2(CH_2)_{1,2}PH_2)_3]^{+2}$, both gold centers are of trigonal planar geometry (P-Au-P ~ 120°). However, for the optimized triplet excited state, in the $[Au_2(PH_2(CH_2)_1PH_2)_3]^{+2}$ model, one of the gold centers has distorted to a T-shape (see Figure. 9a), with P-Au-P angles of (102°, 160°, 98°), while the other gold center retained its original trigonal planar geometry, with angles (116°, 131°, 112°). For the model $[Au_2(PH_2(CH_2)_2PH_2)_3]^{+2}$, the P-Au-P angles were (100°, 160°, 93°) on the distorted gold center, and (122°, 119°, 113°) on the geometry retained center. All Au-P bond distances for either closed model were ~ 2.4 Å. The change in the geometry around one of the gold centers implies that the Au^I dimer in the triplet state is, at least in a conceptual sense, composed of one singlet Au^I and one triplet Au^I centers. The Au---Au distances for closed $[Au_2(PH_2(CH_2)_nPH_2)_3]^{+2}$ were 3.12 Å (singlet, n = 1), 2.88 Å (triplet, n =1); 3.18 Å (singlet, n = 2); 2.87 Å (triplet, n = 2). A crystal structures search was carried on using The Cambridge Crystallographic Data Centre (CCDC),[31] for structures comparable to the models studied in this work. 56 structures with Au---Au distances were found, the average of the Au---Au distances was (2.66 + or – 0.14 Å), with the smallest[32] being (2.52 Å) for the compound bis(benzoate-(μ_2-(2-diethylphosphino)phenylphosphine)-gold(III), and the longest[33] (3.14 Å) for the compound (μ_2-3,5-di-t-butyl-1,2,4-triphospholyl-p,p)-(μ_2-3,5-di-t-butyl-1,2,4-triphospholyl-p,p')-bis(triphenylphosphine-gold(I)). Hence, the already short distances seen in the singlet ground

state of the calculated models are even shorter in the triplet excited state for closed isomer, and commensurate with experimental values reported for Au---Au bonded systems. From the data in Table 3, it can be seen that the closed isomer of the dhpm (dihydrophosphinomethane or $H_2PCH_2PH_2$) model is more stable by 3.2 Kcal/mol versus the open isomer, while the isomer energy preference is reversed for the longer dhpe (dihydrophosphinoethane or $H_2PCH_2CH_2PH_2$) with the open isomer being 16 Kcal/mol more stable than the closed form. This is consistent with experimental literature data.[5,7]

Analyzing the orbital energy levels for the ground state model $[Au_2(PH_2CH_2PH_2)_3]^{+2}$ yielded the diagram (see Figure. 10) which shows the e' pair (symmetry labels appropriate to the D_{3h} point group are used) to be the HOMO, consistent with a Jahn-Teller distortion to a T-shape in the triplet exciton. If the a" was the HOMO as reported previously[14,34] in the literature, then the Jahn-Teller distortion which leads to the T-shape rearrangement would not be expected to occur.

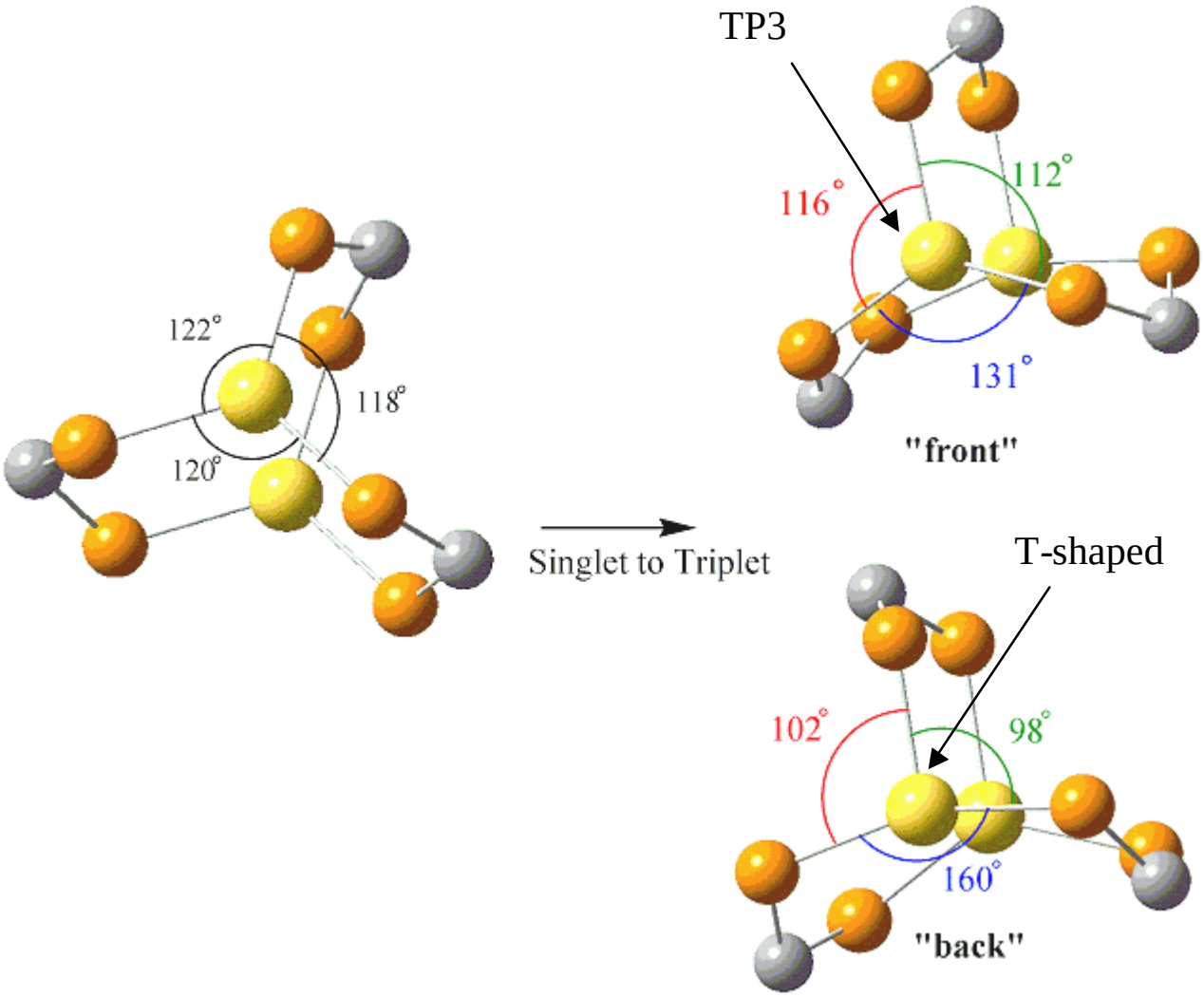

Figure 9a. DFT-optimized geometry of $[Au_2(dhpm)_3]^{+2}$, closed isomer. Hydrogen atoms omitted for clarity.

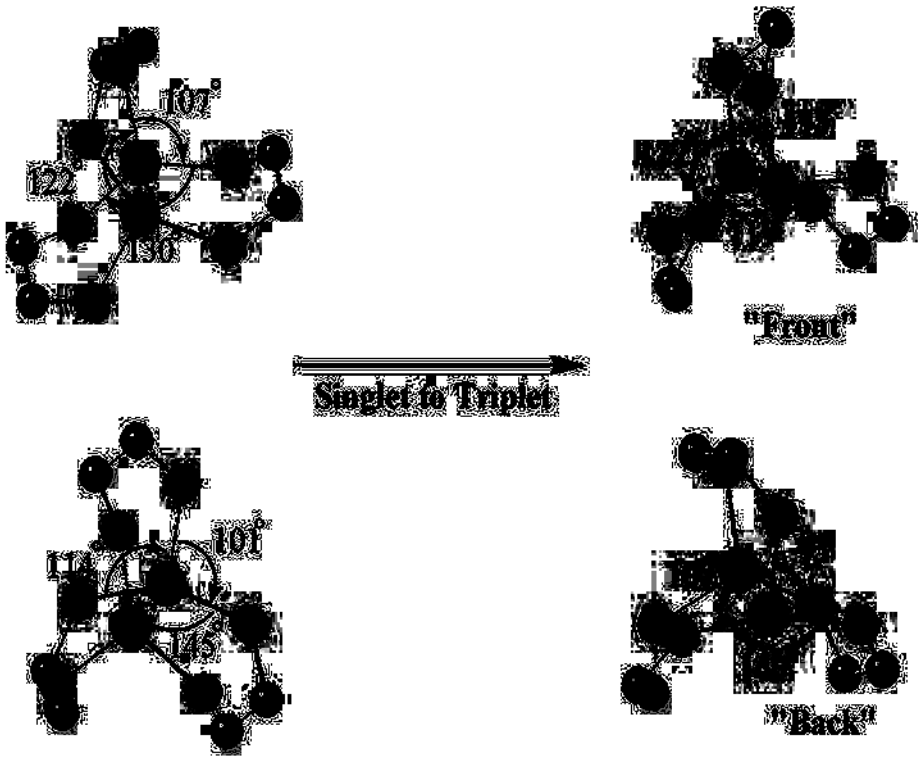

Figure 9b. DFT-optimized geometry of $[Au_2(dhpe)_3]^{+2}$, closed isomer. Hydrogen atoms omitted for clarity.

.

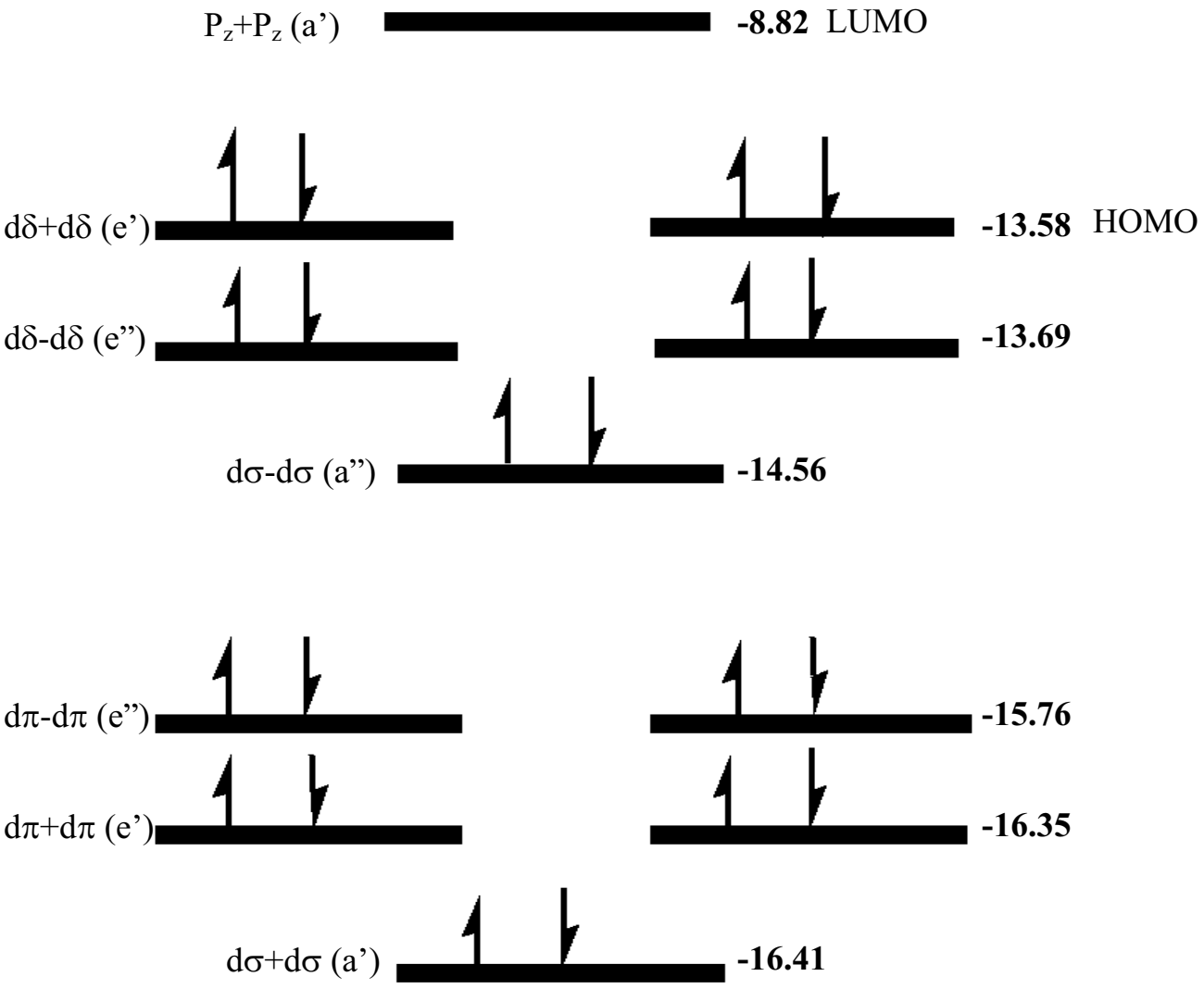

Figure 10. Orbital energy levels (in eV) from a B3PW91 calculation of the singlet ground state of $[Au_2(dhpm)_3]^{+2}$, closed isomer.

CHAPTER 4

SUMMARY, CONCLUSIONS AND PROSPECTUS

Calculations on Au^{I}, Au^{II}, Au^{III}, and Au^{I}-dimer complexes, were carried out using the B3PW91 hybrid functional and relativistic ECPs. The focus of the study was to understand the fundamental nature of the luminescent excited state in gold complexes, in addition to sorting out factors that influence the geometry and bonding properties of gold compounds.

Calculations for Au^{I} complexes (ground state singlet) show that the gold coordination geometry is very dependent on the electronic structure of the ligands: σ-donors yield a linear two-coordinate geometry about the gold, with the third "ligand" dissociated; π-acceptor ligands, phosphines included, are three-coordinate, trigonal planar. No geometries intermediate between the trigonal planar and "T-shaped" could be found by mixing σ-donors and π-acceptors.

Doublet $[Au(PR_3)_3]^{+2}$ distorted to a T-shape geometry, and is thus a ground state model of the triplet exciton of the corresponding $[Au(PR_3)_3]^{+}$ complex. However, for the largest phosphine substituents, Au^{II} complexes have reduced out-of-plane bending about the gold versus triplet $[Au(PR_3)_3]^{+}$. Their distortion towards the T-shape geometry is also less than that for the triplet $[Au(PR_3)_3]^{+}$. Studying the disproportionation of Au^{II} complexes as a function of ligand shows that the reaction is unfavorable (endothermic) for all ligands investigated, and is least endothermic for phosphine and isonitrile (*i.e.*, π-acceptor) ligands. Therefore, $Au^{II}L_3$ complexes containing σ-donor ligands would appear to be worthy experimental targets in the search for gold complexes with novel photochemistry.

For the Au^{I} dimer complexes, the optimized triplet exciton (closed isomer) showed a change in the geometry around one of the gold centers, but not the other. Thus, the dimer exciton is composed of one singlet Au^{I} and one triplet Au^{I} centers. Analyses of the orbitals indicate that

the distortion is of the Jahn-Teller variety. Furthermore, the Au---Au distance is greatly reduced in the excited state versus the ground state, which should yield large Stokes' shifts.

Supported by the presented results, several ideas arise for future research. For Au^{II} complexes, the disproportionation reaction to Au^{I} and Au^{III} species can be further studied by examining equation 3,

$$2\ Au(II)L_3 \leftrightarrow Au(I)L_2 + Au(III)L_4 \qquad (3)$$

influenced by what has been seen for Au^{I} complexes and their preference to forming linear Two-coordinate complexes, and the better suggested square planar geometry for Au^{III} complexes. This analysis can be further enhanced by investigating the effect that would result by adding one ligand at a time to a Au^{II} monomer, up to an $Au^{II}(L_4)$ complex, and possibly applying the same sequence to Au^{I} too. For the Au-dimers, a 2-electron excitation will be studied to examine its effect on the geometry around both Au centers (*i.e.*, distortion towards the T-shape), and explore the effect this excitation would have on the Au---Au distance. Additional calculations are also planned to study the Au^{II}-Au^{II} dimers, to support the results of the previous work, and to provide a model for evaluating the 2-electron excitation study. Also, future calculations will include Au-trimers, the next level of Au complexes to add to the reported results of the monomers and the dimers.

Table 1. $[Au(PH_3)_3]^+$ ground state singlet and excited state triplet calculations using different methodologies and basis sets.

BASIS SET	METHOD	Au-P (Å) Sing.	Au-P (Å) Trip.	P-Au-P (º) Sing.	P-Au-P (º) Trip.
LANL2DZ + P(d)	B3LYP	2.48	2.53 2.73 2.72	120.00	90.16 96.22 173.61
LANL2DZ + P(d) + Au(p)	B3LYP	2.47	2.52 2.71 2.7	119.99	90.64 96.60 172.75
LANL2DZ + P(d) + Au(p)	BLYP	2.48	2.55 2.73 2.75	119.99	91.58 97.50 170.91
LANL2DZ + P(d) + Au(p)	BP86	2.43	2.48 2.65 2.64	120.00	91.11 97.88 171.0
CEP-121G(d) + Au(p)	B3LYP	2.45	2.48 2.65 2.66	119.99	93.19 97.71 169.09
LANL2DZ+P(d) + Au(p)	MP2	2.45	2.45 2.65 2.64	119.99	89.91 95.18 174.90
LANL2DZ+P(d) + Au(p) + Au(2f)	RHF	2.53	2.53 2.82 2.77	119.99	90.13 94.55 175.31
LANL2DZ+P(d) + Au(p) + Au(2f)	B3LYP	2.46	2.48 2.68 2.67	119.99	90.71 96.69 172.59
LANL2DZ+P(d) + Au(p) + Au(2f)	MP2	2.41	2.36 2.42 2.42	120.00	94.26 94.27 153.76
LANL2DZ+P(d) + Au(p) + Au(2f)	B3PW91	2.43	2.43 2.60 2.61	119.99	93.47 93.46 170.04
LANL2DZ+P(d) + Au(p) + Au(2f)	BHANDHLYP	2.46	2.48 2.68 2.67	119.99	90.71 96.69 172.59
LANL2DZ	B3PW91	2.51	2.57 2.75 2.74	119.99	89.23 94.11 176.65

Sing. – singlet state; Trip. – triplet state; P(d) – d polarization function on phosphorus atoms; Au(2f) – diffuse and compact f functions of Pyykkö;[13] Au(p) – Couty-Hall p function;[19] See Computational Methods for further discussion of the methods and basis sets.

Table 2. B3PW91-optimized $Au^{I}L_3$ singlet state, $Au^{II}L_3$ doublet state, and $Au^{III}L_3$ singlet state complexes.

$Au(I)L_3$										
L	B. F.	E(au)	H(au)	G(au)	r (Å)			< (°)		
Terpy	238	-877.4530	-877.2056	-877.2640	2.13	2.32	2.13	76	152	76
Py_3	246	-879.8895	-879.5950	-879.6687	2.03	3.56	2.03	87	180	93
$(HCN)_3$	114	-415.4858	-415.4192	-415.4701	1.99	2.85	1.99	93	174	93
$(MeCN)_3$	153	-533.4530	-533.2940	-533.3628	1.99	2.86	1.99	93	174	93
$(MeNC)_3$	153	-533.3842	-533.2246	-533.2934	2.07	2.06	2.06	120	120	120
$(CO)_3$	108	-475.1116	-475.0795	-475.1270	2.07	2.07	2.07	120	120	120
NCN	153	-533.4440	-533.2844	-533.3552	Au-N 2.83	Au-C 1.93	Au-N 2.06	N-Au-C 103	C-Au-N 172	N-Au-N 84
CCN	153	-533.4261	-533.2662	-533.3351	Au-C 1.98	Au-C 1.98	Au-N 2.87	C-Au-N 94	N-Au-C 93	C-Au-C 173
$Au(II)L_3$										
Terpy	238	-877.0807	-876.8324	-876.8903	2.07	2.07	2.07	80	160	80
$(HCN)_3$	114	-414.9912	-414.9242	-414.9721	2.01	2.18	2.01	95	170	95
$(MeNC)_3$	153	-532.9584	-532.7983	-532.8639	2.03	2.10	2.03	97	166	97
$(CO)_3$	108	-474.5411	-474.5082	-474.5543	2.06	2.15	2.06	96	168	96
$Au(III)L_3$										
Terpy	238	-876.4399	-876.1951	-876.2563	2.22	2.37	2.22	72	143	72
$(HCN)_3$	114	-414.2494	-414.1831	-414.2287	1.97	1.92	1.97	93	175	93
$(MeNC)_3$	153	-532.3216	-532.1630	-532.2257	2.02	1.94	2.02	92	176	92
$(CO)_3$	108	-473.7243	-473.6906	-473.7342	2.09	1.97	2.09	90	179	90

L – ligand; B. F.- Basis functions; (au) – atomic units; E – electronic energy; H – sum of electronic and thermal enthalpies; G – sum of electronic and thermal free energies, (all energies calculated at 1 atm and 298.15 K); r (Å) – Au-L distance in Angstrom units; < (°) – L-Au-L angle in degrees; Terpy – terpyridine; Py – pyridine; NCN – $[Au(CH_3CN)_2(CH_3NC)]^{+1}$, and CCN – $[Au(CH_3CN)(CH_3NC)_2]^{+1}$

Table 3. B3PW91-optimized Au^{I}-dimers.

Model	H (au)	G (au)	E (au)	r Au-Au (Å)	Multip.
Closed					
$Au_2(dhpm)_3$	-434.7061	-434.7809	-434.9315	3.12	1
$Au_2(dhpm)_3$	-434.6018	-434.6749	-434.8256	2.88	3
$Au_2(dhpe)_3$	-552.5034	-552.5891	-552.8197	3.18	1
$Au_2(dhpe)_3$	-552.4070	-552.4903	-552.7220	2.87	3
Open					
$Au_2(dhpm)_3$	-434.7025	-434.7842	-434.9264	6.55	1
$Au_2(dhpe)_3$	-552.5298	-552.6194	-552.8452	7.71	1

(au) – atomic units; E – electronic energy; H – sum of electronic and thermal enthalpies; G – sum of electronic and thermal free energies, (all energies calculated at 1atm and 298.15 K); r Au-Au (Å) – Au-Au distance in Angstrom units; Multip – spin multiplicity; dhpm – dihydrophosphinomethane; dhpe – dihydrophosphinoethane; See Figure 1 for description of open and closed isomer forms.

REFERENCES

1 Pyykkö, P. *Chem. Rev.* 1988, 88, 563.

2 Pyykkö, P. *Angew. Chem. Int. Ed.* 2002, 41, 3573.

3 Vickery, J. C.; Olmstead, M. M.; Fung, E. Y.; Balch, A. L. *Angew. Chem. Int*. Ed. 1997, 36, 1179. Fung, E. Y.; Olmstead, M. M.; Vickery, J. C.; Balch, A. L. *Coord. Chem. Rev.* 1998, 171, 151.

4 Gimeno, M. C.; Laguna, A. *Chem. Rev.* 1997, 97, 511.

5 McCleskey, T. M.; Gray, H. B. *Inorg.Chem.* 1992, 31, 1733.

6 King, C.; Khan, M. N. I.; Staples, R. J.; Fackler Jr., J. P. *Inorg. Chem.* 1992, 31, 3236. Forward, J. M.; Assefa, Z.; Fackler Jr, J. P. *J. Am. Chem. Soc.* 1995, 117, 9103. Assefa, Z.; Forward, J. M.; Grant, T. A.; Staples, R. J.; Hanson, B. E.; Mohamed, A. A.; Fackler Jr, J. P. *Inorg. Chem. Acta.* 2003, 352, 31.

7 Brandys, M.; Puddephatt, R. *J. Am. Chem. Soc.* 2001, 123, 4839.

8 Komiya, S.; Albright, T. A.; Hoffmann, R.; Kochi, J. K. *J. Am. Chem. Soc.* 1976, 98, 7255.

9 Laguna, A.; Laguna, M. *Coord. Chem. Rev*. 1999, 193-195, 837., and references therein.

10 Walker, N.; Wright, R.; Barren, P.; Murrell, J.; Stace, A. *J. Am. Chem. Soc*. 2001, 123, 4223.

11 Blake, A. J.; Gould, R. O.; Greig, J. A.; Holder, A. L.; Hyde, T. I.; Schröder, M. *J. Chem. Soc., Chem. Commun*. 1989, 876. Blake, A. J.; Greig, J. A.; Holder, A. L.; Hyde, T. I.; Taylor, A.; Schröder, M. *Angew. Chem. Int. Ed. Engl.* 1990, 29, 197.

12 Barakat, K.; Cundari, T.; Omary, M. *J. Am. Chem. Soc*. 2003, 125, 14228.

13 Pyykkö, P.; Mendizabal, F. *Inorg. Chem*. 1998, 37, 3018.

14 Yam, V.; Lo, K. *Chem. Soc. Rev*. 1999, 28, 323

15 Harvey, P.; Gray, H. *J. Am. Chem. Soc*. 1988, 110, 2145.

16 Parr, R. G.; Yang, W. *Density-functional Theory of Atoms and Molecules*, Oxford Univ. Press, Oxford, 1989.

17 Becke, A. D. *J. Chem. Phys*. 1993, 98, 5648. Burke, K.; Perdew, J. P.; Wang, Y. *Electronic Density Functional Theory: Recent Progress and New Directions*. Dobson, J. F.; Vignale, G.; Das, M. P. Eds. Plenum, New York, 1998.

18 Hay, P. J.; Wadt, W. R. *J. Chem. Phys*. 1985, 82, 270.

19 Couty, M.; Hall, M. B. *J. Comp. Chem*. 1996, 17, 1359.

20 Vreven, T.; Morokuma, K. *J. Comp. Chem*. 2000, 21, 1419.

21 Rappé, A. K.; Casewit, C. J.; Colwell, K. S.; Goddard III, K. S.; Skiff, W. M. *J. Am. Chem. Soc*. 1992, 114, 10024.

22 Frisch, M. J.; Trucks, G. W.; Schlegel, H. B.; Scuseria, G. E.; Robb, M. A.; Cheeseman, J. R.; Zakrzewski, V. G.; Montgomery, Jr., J. A.; Stratmann, R. E.; Burant, J. C.; Dapprich, S.; Millam, J. M.; Daniels, A. D.; Kudin, K. N.; Strain, M. C.; Farkas, O.; Tomasi, J.; Barone, V.; Cossi, M.; Cammi, R.; Mennucci, B.; Pomelli,C.; Adamo, C.; Clifford, S.; Ochterski, J.; Petersson, G. A.; Ayala, P. Y.; Cui, Q.; Morokuma, K.; Rega, N.; Salvador, P.; Dannenberg, J. J.; Malick, D. K.; Rabuck, A. D.; Ragavachari, K.; Foresman, J. B.; Cioslowski, J.; Ortiz, J. V.; Baboul, A. G.; Stefanov, B. B.; Liu, G.; Liashenko, A.; Piskorz, P.; Komaromi, I.; Gomperts, R.; Martin, R. L.; Fox, D. J.; Keith, T.; Al-Laham, M. A.; Peng, C. Y.; Nanayakkara, A.; Challacombe, M.; Gill, P. M. W.; Johnson, B.; Chen, W.; Wong, M. W.; Andres, J. L.; Gonzalez, C.; Head-Gordon, M.;

Replogle, E. S.; Pople, J. A. Gaussian 98, Revision A.11.3. , Gaussian, Inc., Pittsburgh PA 2002.

23 http://www.gaussian.com/gvw_req.htm.

24 http://www.wavefun.com. SPARTAN'02, Wavefunction, Inc., 18401 Von Karman Avenue, Suite 370, Irvine, CA 92612.

25 MOE – Molecular Operating Environment, Chemical Computing Group, Inc., 1255 University St., Suite 160, Montreal, Quebec, Canada, H3B 3X3.

26 Stratmann, R. E.; Scuseria, G. E.; Frisch, M. J. *J. Chem. Phys*. 1998, 109, 8218.

27 Cotton, F. A; Wilkinson, G. *Advanced Inorganic Chemistry*, Fifth Ed., John Wiley & Sons, INC, NY. 1988, 948-951.

28 Korgaonkar, A. V.; Gopalaraman, C. P.; Rohatgi, V. K. *Inter. J. of Mass Spec and Ion Phys*. 1981, 40, 127.

29 Cammi, R.; Mennucci, B.; Tomasi, J. *J. Phys. Chem.* 2000, A104, 5631. Cossi, M.; Scalmani, G.; Rega, N.; Barone, V. *J. Chem. Phys.* 2002, 117, 43., and references therein.

30 Bensch, W.; Prelati, M.; Ludeig, W. *Chem. Commun*. 1986, 1762.

31 Allen, F. H.; Kennard, O. *Chem. Design. Autom. News*. 1993, 8, 31.

32 Bennett, M. A.; Bhargava, S. K.; Hockless, D. C. R.; Welling, L. L.; Willis, A. C. *J. Am. Chem. Soc*. 1996, 118, 10469.

33 Hofmann, M.; Heinemann, F. W.; Zenneck, U. *J. Organomet. Chem*. 2002, 643, 357.

34 Jaw, H. C.; Savas, M. M.; Mason, W. R. *Inorg. Chem.* 1989, 28, 4366.